Normal Mode Rossby Waves and Their Effects on Chemical Composition in the Late Summer Stratosphere

D. Pendlebury*, T. G. Shepherd*, M. Pritchard*†, and C. McLandress*
*University of Toronto, Toronto, Canada, †now at University of California, San Diego, USA

Introduction

- The Middle Atmosphere Nitrogen TRend Assessment (MANTRA) campaign measures stratospheric chemical species relevant to ozone depletion from balloon-borne instruments during late summer over Vanscoy, Saskatchewan (52°N, 253°E) from 10 to 50 km. It is important to characterize large-scale variability due to planetary waves since it can an impact on chemical species, and on determining long-term trends.
- One source of large-scale variability in the atmosphere is normal mode Rossby waves, which are planetary-scale oscillations. Their spatial structure and phase speeds are determined by the resonance properties of the atmosphere.
- The westward travelling 5-day, 10-day and 16-day waves correspond to the first three gravest, latitudinally anti-symmetric modes with zonal wavenumber 1 (e.g. Salby, 1981).

Mode	5-day	10-day	16-day
Period	4.4-5.7 days	8.3-10.6 days	11.1-20 days
Peak Amp.	50N/S	50N/S	50N/S

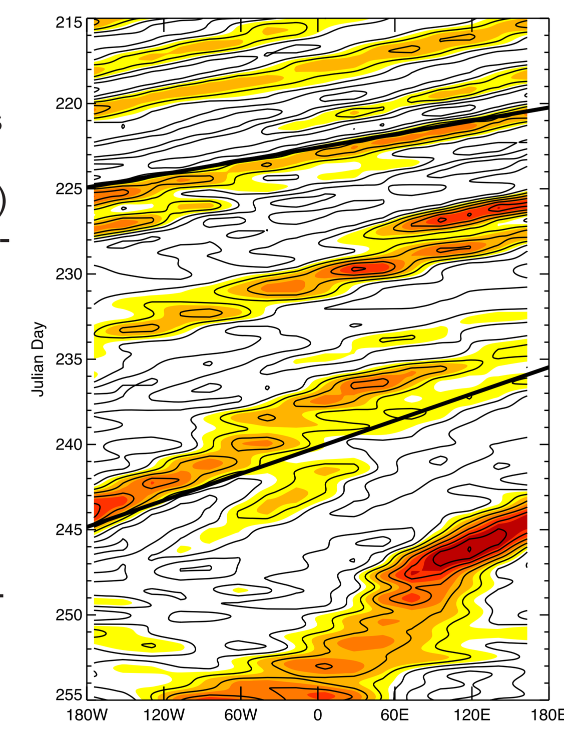

Figure 1: Hovmoller plot of nitrous oxide at 62 km and 52°N. Contour intervals are 1.2 K and higher values are shaded. Overlaid are the phase lines for a wave with period 5 days (top) and 10 days (bottom). Julian days range from 215 (August 3) to 255 (September 12). Contour intervals are 0.03 ppbv.

Model and Analysis

- The Canadian Middle Atmosphere Model (CMAM) is a general circulation model with fully interactive chemistry with a resolution T32 and 50 vertical levels from the ground to 0.0006 mb (~100 km). Two data sets from the same climate simulation are used.
- The first data set has high temporal sampling but sampled only at 16 evenly-spaced longitudes at 52.6°N for a single late-summer period. It will be used to examine the time evolution of the 5-, 10- and 16-day waves over the summer, and to determine the relationship of the waves in the dynamical fields to the chemical fields nitrous oxide (N2O), methane (CH4), and ozone (O3). Waves with periods less than 1.2 days and zonal wavenumbers greater than 4 are filtered to remove any smaller-scale variability and noise. Figure 1 shows the Hovmoller plot of N2O (filtered).
- The second data set has 18 hour sampling for a 24 year period (chemical fields are saved only every 3 days) at all horizontal gridpoints on 5 pressure levels, which will be referred as the global data set. It is used to examine the interannual variability of the wave amplitudes in the dynamical fields.

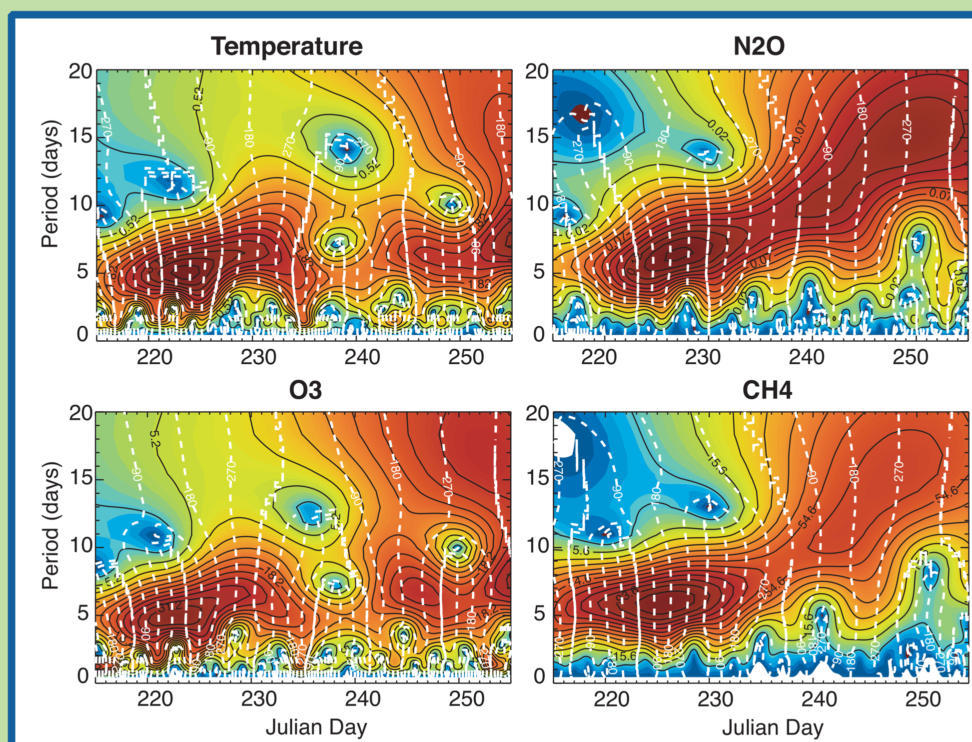

Figure 2: Fourier-wavelet decomposition for temperature (top-left panel), nitrous oxide (top-right panel), ozone (bottom-left panel) and methane (bottom-right panel) at 62 km and 52.6°N. Contour intervals are 0.26 K/km/cpd for temperature, 0.01 ppbv/km/cpd for nitrous oxide, 7.8 ppbv/km/cpd for methane, and 2.6 ppbv/km/cpd for ozone. Phase lines are overlaid for phases 0, 90, 180, and 270.

Seasonal Variation

- The Hovmoller plot for nitrous oxide (Figure 1) at ~62 km for the period August 3 to September 12 clearly shows a wavenumber 1 wave with a westward phase propagation. The disturbance has a period of 5-7 days in mid- to late August (Julian days 220-235). The period then lengthens to ~10 days by late August to early September (Julian days 240-245), and by mid-September is closer to 16 days.
- Because of the temporal variation of the wave period, spectral analysis was done using Fourier decomposition in the zonal direction, retaining only wavenumber 1, and then using wavelet decomposition in time with a Morlet wavelet of order 3. The wavelet analysis is shown in Figure 2 for all four fields at 62 km. In all fields, waves with periods of approximately 5-7 days are present at the beginning of August (Julian day 215), in agreement with the Hovmoller plots.
- The Fourier-wavelet decomposition is integrated over a frequency range for each wave; for the 5-day wave: 1.37-0.97 cpd (cycles per day) (periods of 4.6 to 6.5 days), 10-day wave: 0.68-0.53 cpd (periods of 9.2 to 11.9 days), and 16-day wave 0.44-0.34 cpd (periods of 14.1 to 18.3 days). (See Figure 3.) Because the MANTRA campaign measures at altitudes ranging from 10 km to 50 km, we will focus on the maxima near 50 km.

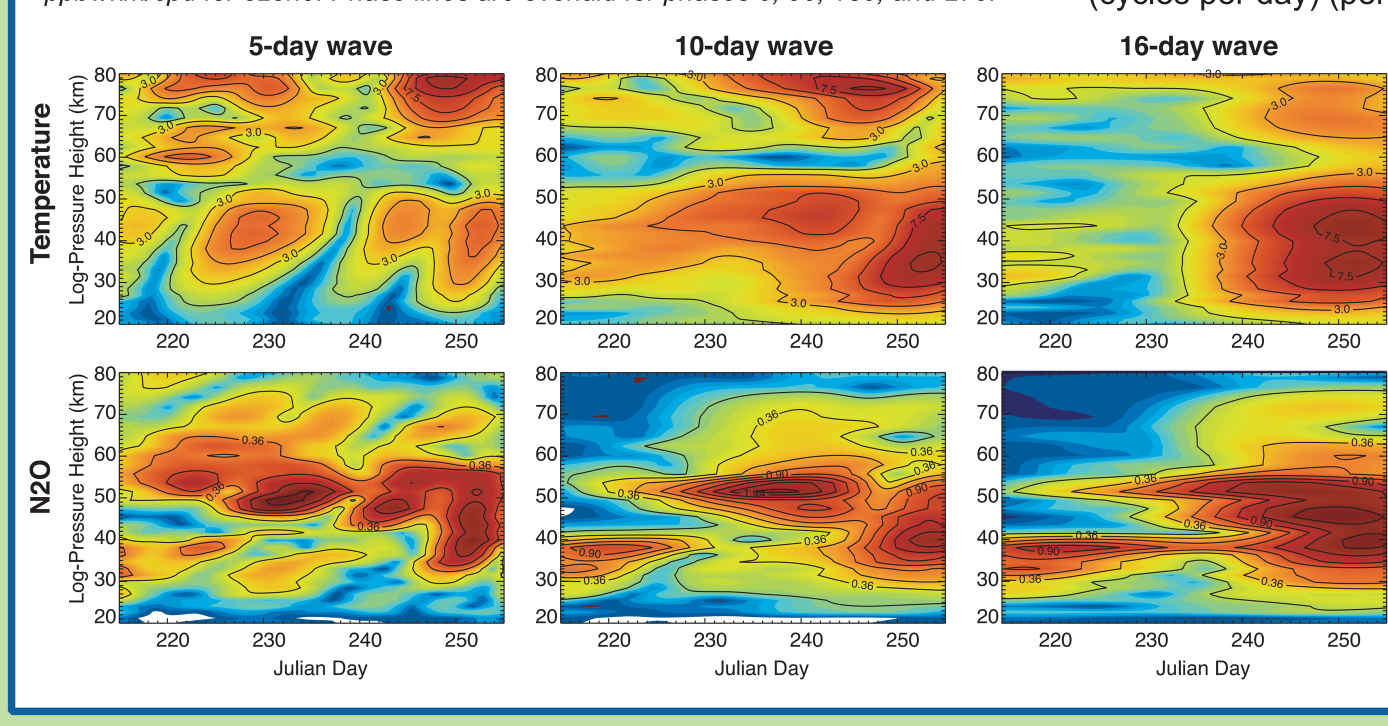

Figure 3: Fourier-wavelet decomposition showing altitude vs. time for temperature (top row) and nitrous oxide (bottom row) for the 5-day wave (left column), 10-day wave (middle column) and 16-day wave (right column). Contour intervals are 1.5 K/km/cpd for temperature, and 0.18 ppmv/km/cpd for nitrous oxide. Nitrous oxide has been scaled by a density factor of ρ(1000mb)/ρ(p). Methane and ozone show similar behaviour.

The zonal-mean zonal wind at 52.6°N may provide some explanation for the lengthening of the wave period. Figure 4 shows the zonal-mean zonal wind evolution over the late summer period, and the critical lines for westward travelling waves with zonal wavenumber 1 and periods of 5, 10 and 16 days. As suggested by Geisler and Dickinson (1976) and Prata (1989) for the 5-day wave, the waves become vertically trapped by the easterly jet. As the zonal-mean zonal wind approaches turnaround, the area of allowed horizontal propagation (below the critical levels) grows as the jet weakens.

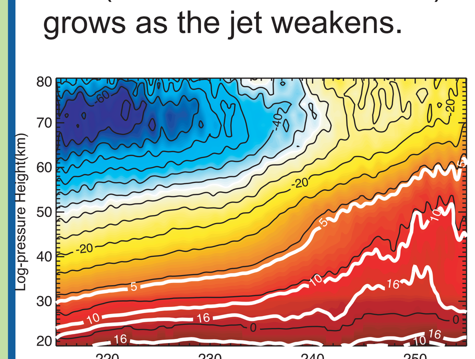

Figure 4: The zonal-mean zonal wind at 52.6°N from August 3 to September 12. Contour levels are 5 m/s and reach a minimum of −73.3 m/s. Thick white lines represent the critical lines for planetary waves with zonal wavenumber one and periods of 5, 10 and 16 days, labelled accordingly.

Correlations

- Time-lagged correlations of temperature versus nitrous oxide, methane and ozone are shown in Figure 5. Where the time-lag is positive, the changes in the temperature lead changes in the chemical fields, and where it is negative, the chemical fields lead temperature. However, due to the periodic nature of the 5-, 10- and 16-day waves, causality is not implied by the sign of the lag.
- Between 28 and 33 km, where the chemical lifetimes of these species are longer than transport time scales, transport is expected to be dominant in controlling the chemical distributions. Further investigation reveals that the correlations in this region are in part due to meridional transport: the nitrous oxide and methane are weakly positively correlated with meridional wind at these heights.
- Above, where chemical lifetimes are shorter, chemistry becomes more important. Ozone is anti-correlated with temperature with a zero time-lag, suggesting that it adjusts almost simultaneously to the temperature in this region. The role of chemistry should be less important for nitrous oxide and methane, which both have lifetimes of several months at these altitudes.
- Time-lagged correlations for the 5-, 10- and 16-day waves are shown in Figure 6. The periodicity of the time series is clearly reflected in the periodic nature of the correlations. However, caution must also be used in interpreting these results. For example, although there appears to be a significant correlation between temperature and nitrous oxide, and between temperature and ozone at 60 km with a time lag of -1 day, the amplitude of the 10-day wave is very small at this altitude. Therefore, the 10-day wave may not significantly affect the chemical concentrations in this region.
- Correlations with the waves in the meridional wind field (not shown) suggest that the links between temperature and nitrous oxide, and methane between 30 km and 60 km are partly due to meridional transport. The relationship between temperature and ozone for the waves appears to be partly through transport and partly through a chemical balance between temperature and ozone.

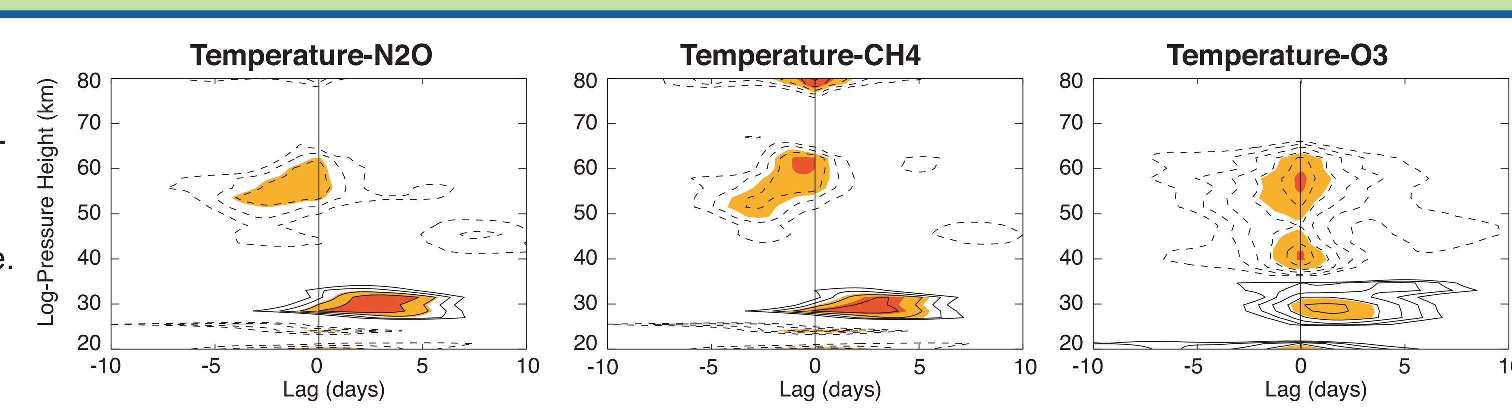

Figure 5: Time-lagged correlations of temperature and nitrous oxide (left panel), temperature and methane (middle panel), and temperature and ozone (right panel). Contours are 0.05 and are shown only for |CorXY| > 0.5. Significance levels for the 90% (yellow), 95% (orange) and 99% (red) are shown.

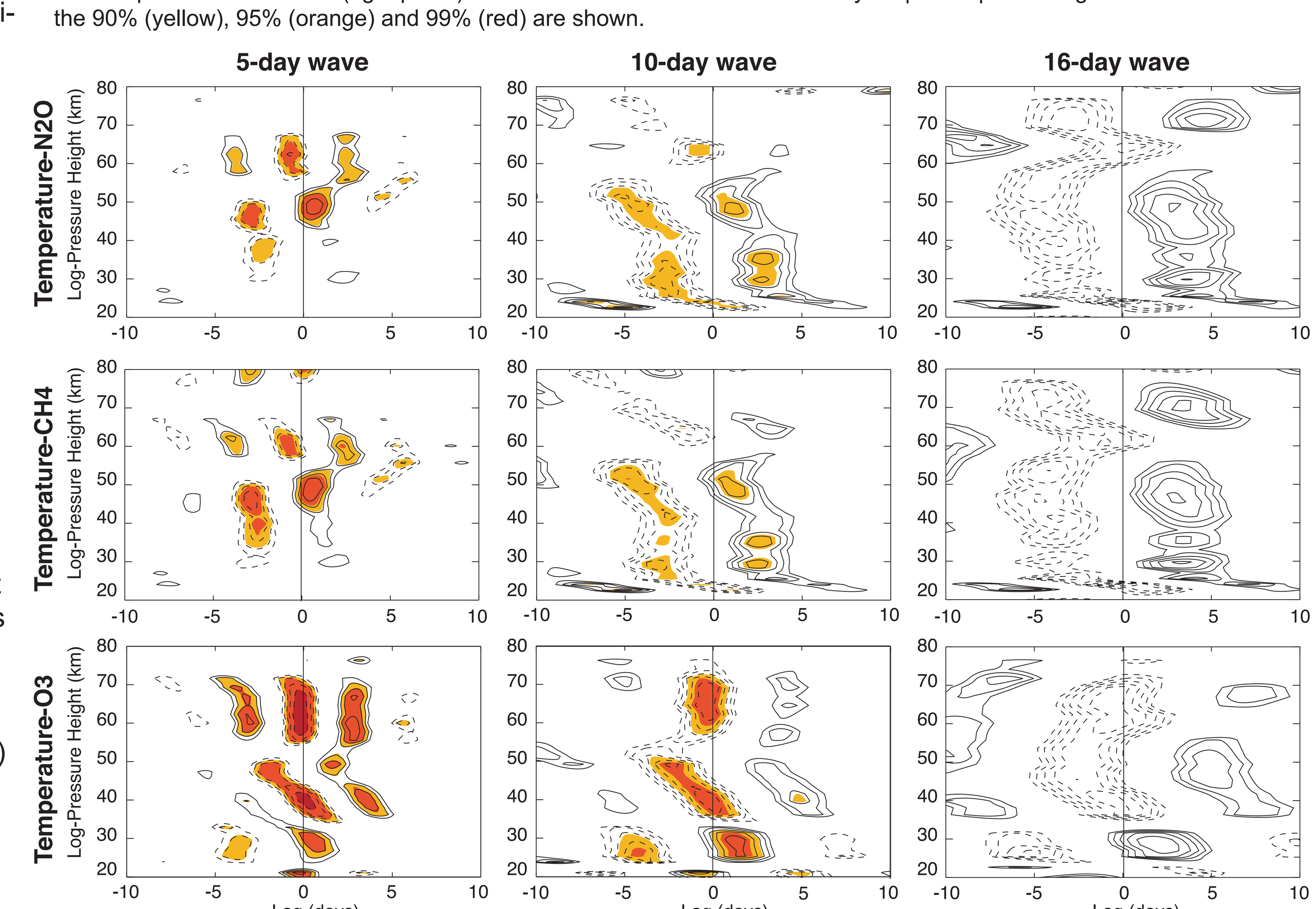

Figure 6: Similar to Fig. 6 but for correlations between temperature-N2O (top row), temperature-CH4 (middle row) and temperature-O3 (bottom row) for the 5-day (left column), 10-day (middle column) and 16-day waves (right column).

References

Geisler, J. E. and Dickinson, R. E.: The five-day wave on a sphere with realistic zonal winds, *J. Atmos. Sci.*, **33**, 632–641, 1976.

Madden, R. and Julian, P.: Further evidence of global-scale, 5-day pressure waves, *J. Atmos. Sci.*, **29**, 1464–1469, 1972.

Pendlebury, D., T. G. Shepherd, M. Pritchard and C. McLandress, Normal mode Rossby waves and their effects on chemical composition on the late summer stratosphere, *Atmos. Chem. Phys.*, **8**, 1925-1935, 2008.

Prata, A. J.: Observations of the 5-day wave in the stratosphere and mesosphere, *J. Atmos. Sci.*, **46**, 2473–2477, 1989.

Salby, M. L.: Rossby normal modes in nonuniformbackground configurations. Part II: Equinox and solstice conditions, *J. Atmos. Sci.*, **38**, 1827–1840, 1981.

Sciremammano, F., J.: A suggestion for the presentation of correlations and their significance levels, *J. Phys. Ocean.*, **9**, 1273–1276, 1979.

Interannual variability

- Although the 5-day, 10-day and 16-day waves are resonant modes of the atmosphere, all are expected to exhibit some interannual variability since the resonant properties of the atmosphere change with varying background winds and temperatures, which themselves exhibit interannual variability.
- In order to characterize the interannual variability of the waves, model data from 24 years of the global data set sampled at 18 hour intervals on five pressure levels for the months of August and September were used.The Fourier-wavelet decomposition is used to isolate the waves, and amplitudes are again integrated over period ranges 4.6-6.5 days (5-day wave), 8.4-10.9 days (10-day wave) and 14.2-18.4 days (16-day wave). Results for a typical year are shown in Figure 9.
- To examine the year-to-year variability of the waves, the amplitudes were integrated over the latitude range 39°N to 72°N. (Not shown)
- For both the 10- and 16-day waves, the amplitude tends to grow more steadily over the summer, whereas the 5-day wave amplitude shows the greatest variation in timing. As noted earlier, interpretation of the 10-day wave is difficult because of the overlap of periods between it and the 5 and 16 day waves.

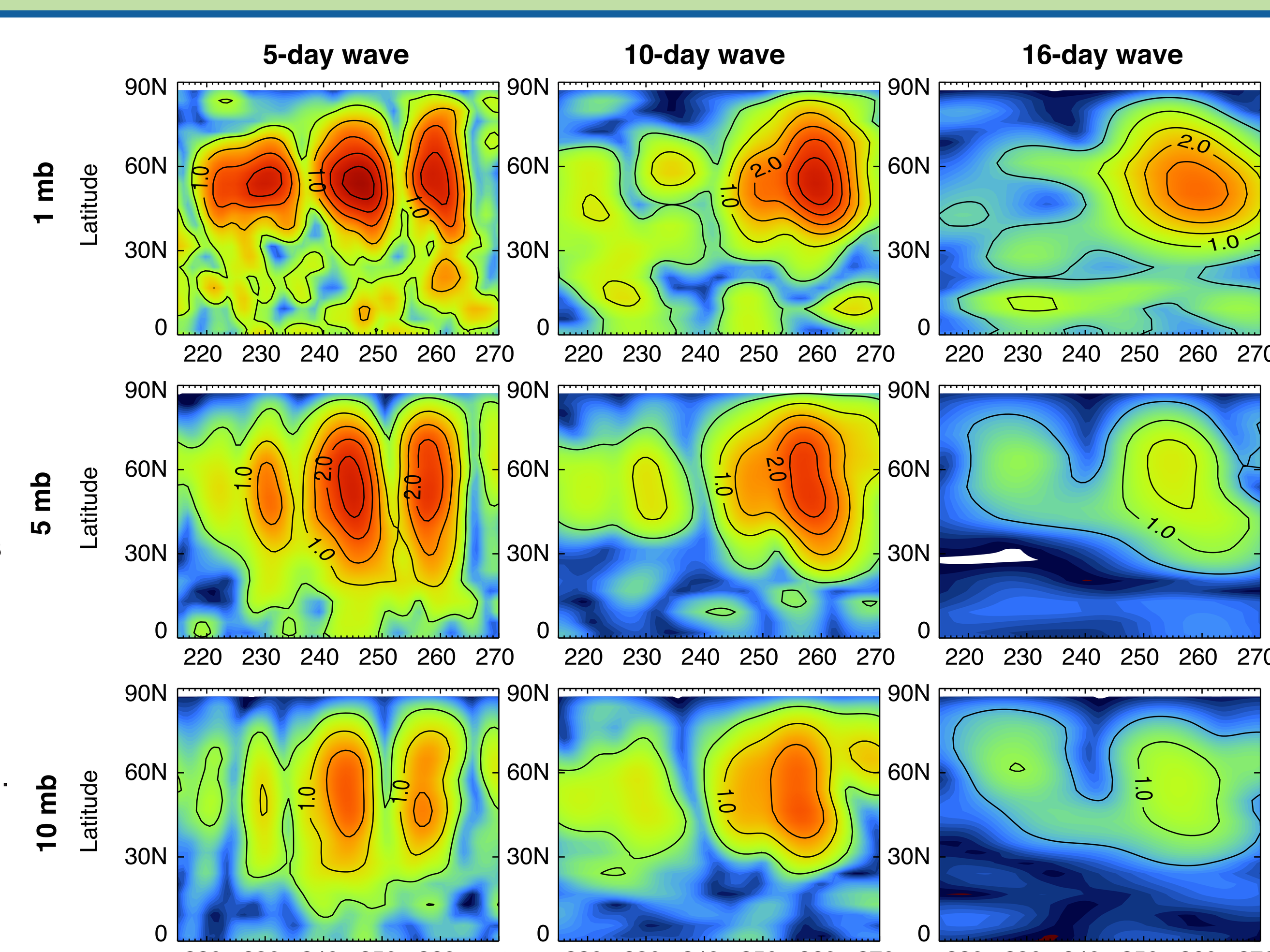

Figure 7: Temperature amplitudes as calculated for Figure 4, but for year 17 of the global data set. Amplitudes are shown for the NH only for the 5-day wave (left column), 10-day wave (middle column), and 16-day wave (right) column for pressure levels 1 mb (~48 km) (top row), 5 mb (~35 km) (middle row) and 10 mb (~32 km) (bottom row). Contour intervals are 0.5 K/km/cpd in all panels.

Discussion and Conclusions

- Using the CMAM, the normal mode Rossby waves for the 5-, 10- and 16-day waves in both the temperature and chemical fields have been analysed. All fields are shown to have 5-, 10- and 16- day waves, and there is a clear correlation between the temperature, nitrous oxide, methane and ozone.
- The relationships between the waves in the dynamical and chemical fields are surprisingly complicated. For a long-lived tracer advected purely by the meridional velocity v of a given wave, a 90° phase lag (e.g. 4 days for the 16-day wave) would be expected between v and the tracer. The results here show that the phase relationships between v and temperature, and temperature and the tracers vary in time and height, so it would seem that meridional transport is not the only active process.
- Advection of the chemical species by the vertical winds may play a role, but this hypothesis cannot be tested with the existing data set, since no information pertaining to the meridional structure is available.
- This study suggests that the variability in chemical constituents induced by Rossby waves in the summer stratosphere should be taken into account when estimating long-term trends from the MANTRA campaigns. Our examination of the interannual variability of the 5-,10- and 16- day waves shows that these waves could, and likely do, exist in August and September.

Acknowledgements

The authors would like to thank Stella Melo and David Sankey for initial discussions. Publication of this work was supported by the Canadian Foundation for Climate and Atmospheric Sciences.